# Author's Accepted Manuscript

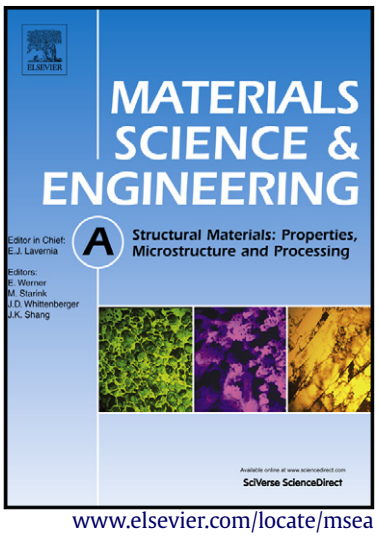


www.elsevier.com/locate/msea

Surface nanocrystallization of Cu and Ta by sliding friction

Y.S. Zhang, P.X. Zhang, H.Z. Niu, C. Chen, G. Wang, D.H. Xiao, X.H. Chen, Z.T. Yu, S.B. Yuan, X.F. Bai

PII: S0921-5093(14)00380-3
DOI: http://dx.doi.org/10.1016/j.msea.2014.03.089
Reference: MSA30938

To appear in: *Materials Science & Engineering A*

Received date: 24 January 2014
Revised date: 24 March 2014
Accepted date: 25 March 2014

Cite this article as: Y.S. Zhang, P.X. Zhang, H.Z. Niu, C. Chen, G. Wang, D.H. Xiao, X.H. Chen, Z.T. Yu, S.B. Yuan, X.F. Bai, Surface nanocrystallization of Cu and Ta by sliding friction, *Materials Science & Engineering A*, http://dx.doi.org/10.1016/j.msea.2014.03.089

# Surface nanocrystallization of Cu and Ta by sliding friction

Y.S. Zhang[a,*], P.X. Zhang[a], H.Z. Niu[a], C. Chen[b], G. Wang[c], D.H. Xiao[d], X.H. Chen[e], Z.T. Yu[a], S.B. Yuan[a], X.F. Bai[a]

[a] *Northwest Institute for Nonferrous Metal Research, Xi'an 710016, China*

[b] *School of Material and Mineral Resources, Xi'an University of Architecture & Technology, Xi'an 710055*

[c] *Centre for Advanced Materials Processing and Manufacturing, The University of Queensland, St Lucia, Queensland 4072, Australia*

[d] *State Key Lab of Powder Metallurgy, Central South University, Changsha 410083, China*

[e] *College of Materials Science and Engineering, Chongqing University, Chongqing 400045, PR China*

*E-mail: y.sh.zhang@163.com*

Optimization of the surface structure and properties is of great concern in that the failures of engineering materials such as wear, erosion and fatigue usually occur on the surface of materials. Plastic deformation from the sliding friction process has been utilized to realize surface nanocrystallization in commercial pure copper and tantalum plates in this work. The optical microscopy, transmission electron microscopy, X-ray photoelectron spectra, and uniaxial tensile testing results suggested that clean nanocrystalline surface layers of pure copper and tantalum were obtained, significantly strengthening the materials after the treatment.

*Keywords:* Nanostructured materials; Non-ferrous alloys; Grain refinement

## 1. Introduction

A new family of severe plastic deformation processes have attracted considerable scientific interests in order to generate nanocrystalline surface layer for bulk materials [1]. Various surface deformation techniques have been developed by transforming the initial coarse-grained (CG) structure of a bulk material into refined-grain structure, such as surface mechanical attrition treatment (SMAT) [1], air blast shot peening [2], wire-brushing [3], and surface mechanical grinding treatment (SMGT) [4]. These advances enhance several types of mechanical properties while keeping the overall chemical composition of the target material unchanged.

Friction is a dissipative process encountered in daily life and industry manufacture. Many experimental results have illustrated that microstructure in the near-surface layer might be changed accordingly during friction and wear process under different contact conditions. Surface microstructure observations showed that plastic deformation could result in the formation of grains with a size falling into nanometer regime. Grains in the surface layer of pure copper with a size less than 60 nm have been found in an early study on subsurface structure of pure copper abrased against SiC paper [5]. After sliding against the zirconia disc, the grain size in the surface of the 316 stainless steel could be refined to 8-23 nm [6]. According to Hughes's experimental results, the average geometrically necessary boundaries were only 10 nm, with nanocrystalline surface layer depth in excess of 4 μm [7]. During friction process, only one tenth of the energy was undertaken by wear, while most of the energy was consumed in deformation, heat and noise et. al [8]. Thus it is supposed

that in case a suitable process is selected, wear loss can be controlled and more energy can be consumed in plastic deformation. A thick nanocrystalline surface layer in excess of 100 μm underneath the worn surface of pure copper induced by sliding against a WC-Co ball by utilizing a generic friction and wear tester has been reported elsewhere by the current authors [9]. These results further experimentally verified sliding friction as a potential approach to create nanocrystalline structures on the surface layer of metallic materials.

As such, we have developed a surface nanocrystallization technology by means of sliding friction treatment (SFT) with a specified device with enlarged sliding amplitude and improved controllable contact condition to scale up sample size. This work described the generation of nanostructured surface layer on pure copper and tantalum by sliding friction process and reported subsequent changes in the mechanical properties of the treated surfaces.

## 2. Experimental procedures

99.95 wt% pure copper and tantalum plates with a size of 200×200×3 $mm^3$ and a roughness of 0.4 μm were annealed at 973 K and 1273 K, respectively, for 60 minutes, in order to eliminate the effect of mechanical processing on the surface and to homogenize the microstructure. The experiments were conducted on a special designed device in a ball-on-disc contact configuration as shown in Fig. 1(a), in which a spherical WC-Co ball of 10 mm in diameter bearing a normal load was static and the specimen (copper or tantalum) subjected to SFT was firmly installed in a table and

pressed together with the WC-Co ball under a preset normal force of 100-500 N. The table moved independently along x and y axis driven by two motors. The sliding of the specimen with an amplitude of 50 mm ($d_1$) at a speed of 0.2 m/s ($v_1$) with respect to the WC-Co ball along x axis were made firstly, then table with the specimen shifted along the y axis for a step of 100 μm ($d_2$), and the sliding process continued until the area on the specimen surface is sliding treated. The sliding was carried out under chlorcosane as lubricant for the tantalum while the copper was conducted under a dry condition in an ambient environment. An image of a Cu sheet after SFT with a surface roughness of 0.7 μm and treated surface area of 100 mm ×150 mm is shown in Fig. 1(b).

The microstructure of the surface layer of the treated samples was characterized by using an Olympus PMG 3 optical microscopy (OM) and a JEOL JEM-2100 transmission electron microscope (TEM) operated at a voltage of 200 kV. Thin foil samples for TEM observations were cut from the treated surface layer and thinned by ion thinning at low temperatures.

X-ray photoelectron spectroscopy (XPS) was carried out on a Thermo Fisher ESCACAB 250XI spectrometer, by using monochromatic Al Ka radiation and detection pass energy ranging between 30 and 100 eV. Argon sputtering was applied at a pressure of $1 \times 10^{-7}$ Pa under a 3 kV beam accelerating voltage.

The as-treated plates were mechanically polished on the top surface to remove 1-2 μm in depth to eliminate the roughness effect on tensile properties. Down-sized tensile specimens shown in Fig. 1(c) were cut with the testing direction along the

sliding direction by using electro-discharging machining. Afterwards, mechanical polishing was performed from back side of the treated sample to a mirror finish with a designed thickness. Tensile tests were performed on a Tytron 250 Microforce Testing System (MTS System Corporation, with a precision of force measurement of 10 mN) at a strain rate $5 \times 10^{-3}$ $s^{-1}$ at room temperature. A contactless MTS LX300 Laser extensometer was used to calibrate and measure the strain of the tested sample during loading.

## 3. Results and discussion

Figure 2 shows the microstructure from longitudinal cross-section of the Cu sample before and after SFT. Plastic deformation and traces of plastic flow are evident in the treated surface layer, instead of the original CG structure. After SFT at 100 N, the topmost deformed subsurface layer features discontinuous in a wave pattern. This is similar to the vortex structure appeared in some local zones of the upmost worn subsurface, which has been usually found [10-12] and checked in details by Yao [13] to be composed of severely refined grains. It is apparent that the plastic flow lines extended to a greater depth as the load increases to 200 N, and the deformed subsurface layer tends to be continuous, with grain boundaries bent towards one direction with decreasing depth toward the surface.

As revealed by TEM morphologies and the corresponding selected area electron diffraction (SAED) pattern in Figs. 2(d) and (e), elongated grains with random crystallographic orientations are formed in the top surface layer of the sample. The

113 average transverse axis grain size ($d_t$) and longitudinal axis grain size ($d_l$) are 60 and
114 110 nm, respectively, although a certain number of grains approaching 200 nm are
115 also present. The grain size is slightly larger than that in the surface layer of the Cu
116 sample subjected to SMGT (22 nm, 45 nm in transverse axis and longitudinal axis
117 size respectively) under liquid nitrogen [4] and SMAT (10 nm) for 30 min [14].

118 Microstructures of the longitudinal cross-sectional Ta sample before and after
119 SFT are presented in Figs. 3(a)-(c). Initial Ta sample has an equiaxed grain structure
120 with size of 30-60 μm (Fig. 3(a)), and after SFT at a load of 200 N, a plastic deformed
121 surface layer with the thickness exceeding 100 μm is formed clearly as shown in Fig.
122 3(b). When sliding load increases to 500 N, the deformation layer of about 300 μm in
123 depth is reached, as revealed in Fig. 3(c). Plastic flow lines are inclined to the surface
124 as they approached the worn surface, similar to the case for Cu in Fig. 2(c). The
125 detailed TEM observations show that roughly equiaxed grains with size ranging from
126 3 to 15 nm and an average grain size of 7 nm are formed in the topmost layer (Figs.
127 3(d) and (e)).

128 Materials in sliding contact develop large plastic strain and strain rate adjacent to
129 the sliding interface in that actual contact took place in some asperities of the friction
130 pair. Plastic shear strains in the range of 10–1000 have been reported [7, 15-17]. For
131 example, based on the volume grain boundary area and von Mises relation, Hughes
132 [17] extrapolated that the strain in the top-surface of copper subjected to friction was
133 roughly 25 and the maximum shear strain rates being up to $5 \times 10^3$ $s^{-1}$. Owing to much
134 high strain and high strain rate, a nanocrystalline structure will be produced, which

had been validated by large-scale molecular dynamics simulations [18] and considerable amounts of experiments over the past several decades [5-7, 19]. Current SFT has induced nanocrystalline structure on the subsurface for both Cu and Ta, and finer grain size for Ta than that for Cu may be attributed to the difficulty in dislocations recovery due to its higher melting temperature.

XPS results (Fig. 4) showed that C and O coming from the mating ball or atmosphere were detected on the treated surface of the Cu and Ta samples, while the impurity contents decreased remarkably away from the surface. For example, after etching 840 s, the C content was decreased by two orders of magnitude for the two samples. The measured values from XPS are summarized in Table 1. It is reasonable to obtain clean nanocrystalline surface layer for Ta because the lubricant oil used could alleviate wear and isolate the air from the contact surfaces. For the metals sliding in air, it is common to produce oxides which are then available to mechanically mix with unoxidized metal to form a mechanically mixed surface layer [16, 20, 21]. In this work, large moving distance up to 50 mm imposed played a dominant role in reducing impurity of the surface layer. Compared with our previous study with a much lower travel distance (0.5 mm), the severe oxidation process and subsequent behavior of oxide debris in between contact surfaces subjected to relative slip will result in the thick oxide layer [22]. While in the present study during the large distance sliding, the heat generated during friction should be radiated easily, which can significantly alleviate oxidation. Moreover, it benefitted for the oxide debris and contamination from transferred materials to be removed from the contact

zone. Consequently, a much thinner contamination layer was generated on the nanostructured surface layer of the treated sample.

Results from uniaxial tensile tests in Fig. 5 showed that the nanocrystalline samples exhibited much higher yield strength (YS) and ultimate tensile strength (UTS) compared with their CG counterparts for both Ta and Cu. The YS of the SFT Cu and SFT Ta have reached 450 MPa and 720 MPa, respectively, which are considerably higher than that of the corresponding CG samples (75 MPa for Cu and 300 MPa for Ta). However, the plasticity was depressed for the nanocrystalline samples, with an elongation-to-failure less than 2% for both materials. It was reasonable that nanocrystalline grains tended to significantly lose work hardening on deformation owing to their very low dislocation storage efficiency inside tiny grains [23]. It was noted that the SFT Cu with a 200 μm in thickness exhibited a YS of 300 MPa and a moderate elongation of 4.4. It was in well agreement with the results in [24] and further verified that an approach using gradient nano-grained layers as advanced coatings of bulk materials could enhance strength-ductility synergy of materials.

## 4. Conclusions

The sliding friction was used to refine the grain structure on the surface of pure Cu and Ta plates with a size scale up to 100 mm × 150 mm. The average grain size in the upmost surface layer of the Cu and Ta can be reduced down to 60 nm and 7 nm respectively. Surface contaminated layer from the ball-disc sliding is reasonably low in depth. The yield strength of the Cu and Ta has been improved from 75 MPa and

300 MPa to 450 MPa and 720 MPa after SFT, respectively. Current study revealed that SFT was a promising process to realize nanocrystalline material surface with a low contamination.

**Acknowledgements**

This work was supported by the National Natural Science Foundation of China (Grants Nos. 50901062 and 51271152) and National Basic Research Program of China (973 Program) (Grant No. 2012CB619102).

**References**

[1] K. Lu, J. Lu, J. Mater. Sci. Technol. 15 (1999) 193-197.

[2] M. Umemoto, Y. Todaka, K. Tsuchiya, Mater. Trans. 44 (2003) 1488-1493.

[3] M. Sato, N. Tsuji, Y. Minamino, Y. Koizumi, Sci. Tech. Adv. Mater. 5 (2004) 145-152.

[4] W.L. Li, N.R. Tao, K. Lu, Scripta Mater. 59 (2008) 546-549.

[5] D.M. Turley, L.E. Samuels, Metallography 14 (1981) 275-294.

[6] W.M. Rainforth, R. Stevens, J. Nutting, Philos. Mag. A 62 (1992) 621-641.

[7] D.A. Hughes, N. Hansen, Phys. Rev. lett. 87 (2001) 135503.

[8] A.A. Hisham, Wear 254 (2003) 884-890.

[9] Y.S. Zhang, W.L. Li, G. Wang, L.C. Zhang, B. Yao, Z. Han, Mater. Lett. 68 (2012) 432-434.

[10] A. Kolubaev, S. Tarasov, O. Sizova, E. Kolubaev, Tribol. Int. 43 (2010) 695-699.

[11] V. Panin, A. Kolubaev, S. Tarasov, V. Popov, Wear 249 (2002) 860-867.

[12] E.V. Legostaeva, Y.P. Sharkeev, Tribol. Int. 39 (2006) 417–425.

[13] B. Yao, Z. Han, K. Lu, Wear 294-295 (2012) 438-445.

[14] Y.S. Zhang, Z. Han, K. Wang, K. Lu, Wear 260 (2006) 942-948.

[15] S. Karthikeyan, H.J. Kim, D.A. Rigney, Phys. Rev. Lett. 95 (2005) 106001.

[16] D.A. Rigney, Wear 245 (2000) 1-9.

[17] D.A. Hughes, D.B. Dawson, J.S. Korellis, L.I. Weingarten, J. Mater. Eng. Perform. 3 (1994) 459-475.

[18] J.E. Hammerberg, B.L. Holian, J. Roeder, A.R. Bishop, S.J. Zhou, Physica D 123 (1998) 330–340.

[19] L. Meshi, S. Samuha, S.R. Cohen, A. Laikhtman, A. Moshkovich, V. Perfilyev, I. Lapsker, L. Rapoport, Acta Mater. 59 (2011) 342-348.

[20] W. Tuckart, L. Iurman, E. Forlerer, Wear 271 (2011) 792-801.

[21] Y.S. Zhang, K. Wang, Z. Han, G. Liu, Wear 262 (2007) 1463-1470.

[22] Y.S. Zhang, Z. Han, K. Lu, Wear 265 (2008) 396-401.

[23] X.H. Chen, J. Lu, L. Lu, K. Lu, Scripta Mater. 52 (2005) 1039-1044.

[24] T.H. Fang, W.L. Li, N.R. Tao, K. Lu, Science 331 (2011) 1587-1590.

**Table 1.** Variations of the element contents (in wt. %) with sputtering time from the treated surface in the SFT samples.

| | SFT Cu | | | |
|---|---|---|---|---|
| | 0 s | 60 s | 240 s | 840 s |
| Cu | 31 | 91.2 | 98.8 | 99.5 |
| O | 22 | 1.89 | 0.35 | 0.11 |
| C | 47 | 6.91 | 0.85 | 0.39 |
| | SFT Ta | | | |
| | 0 s | 60 s | 240 s | 840 s |
| Ta | 35.55 | 82.5 | 95.68 | 98.61 |
| O | 29.35 | 16.16 | 3.46 | 1.34 |
| C | 35.1 | 1.34 | 0.86 | 0.25 |

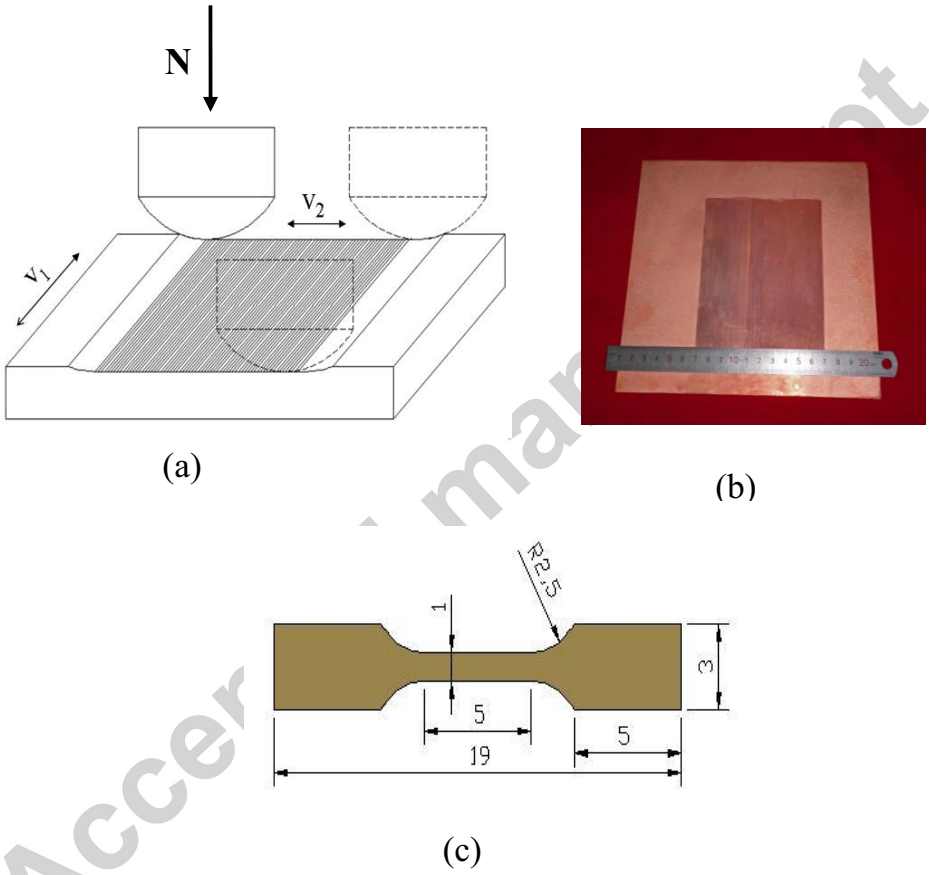


**Figure 1.** (a) Schematic illustrations of the sliding friction treatment set-up, (b) a photograph of a Cu sheet after sliding friction treatment and (c) the geometry of the tensile specimen.

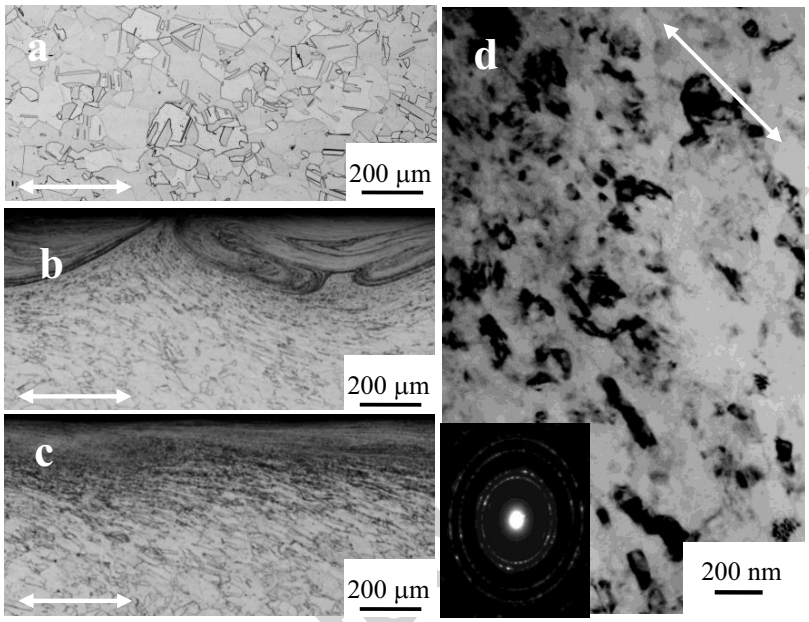


**Figure 2.** Cross-sectional optical images of (a) the original and SFT Cu samples under load of (b) 100 N and (c) 200 N, (d) a bright-field TEM image and a corresponding SAED insert showing the microstructure at the topmost surface in (c). Doubly pointed arrow indicates the sliding direction.

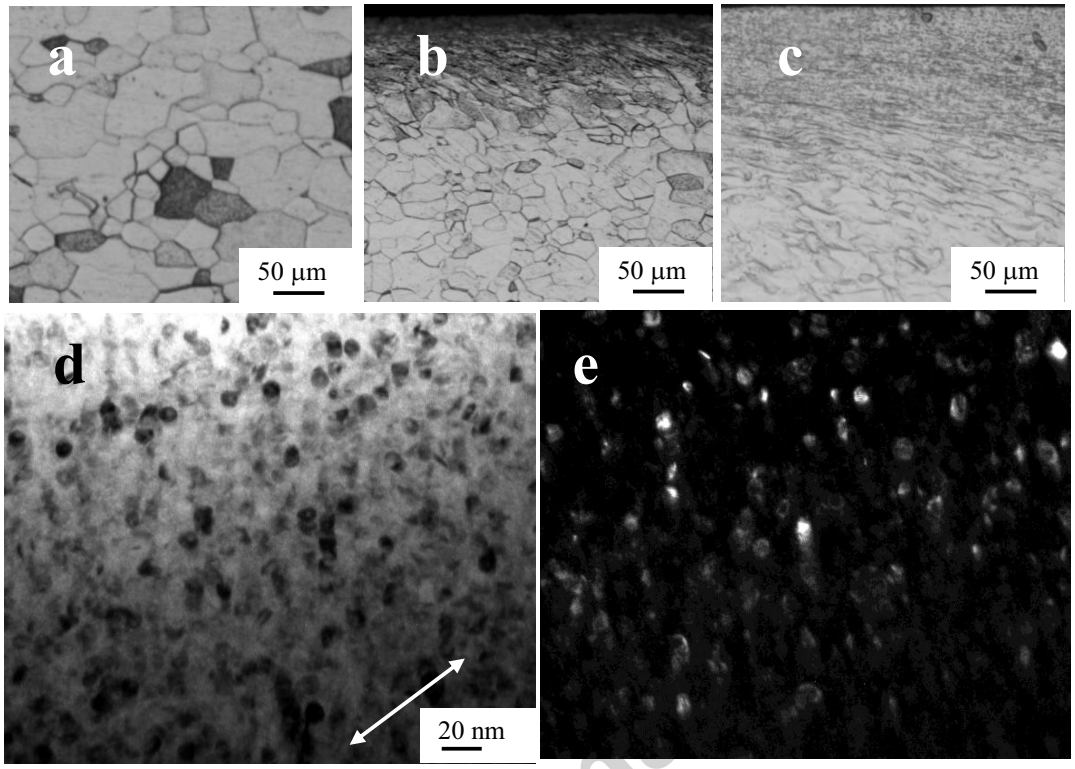


**Figure 3.** Cross-sectional optical images of (a) the original and SFT Ta samples under load of (b) 200 N and (c) 500 N. (d) A bright-field TEM image and (e) a dark-field TEM image showing the microstructure at the topmost surface layer in (c). Doubly pointed arrow indicates the sliding direction.

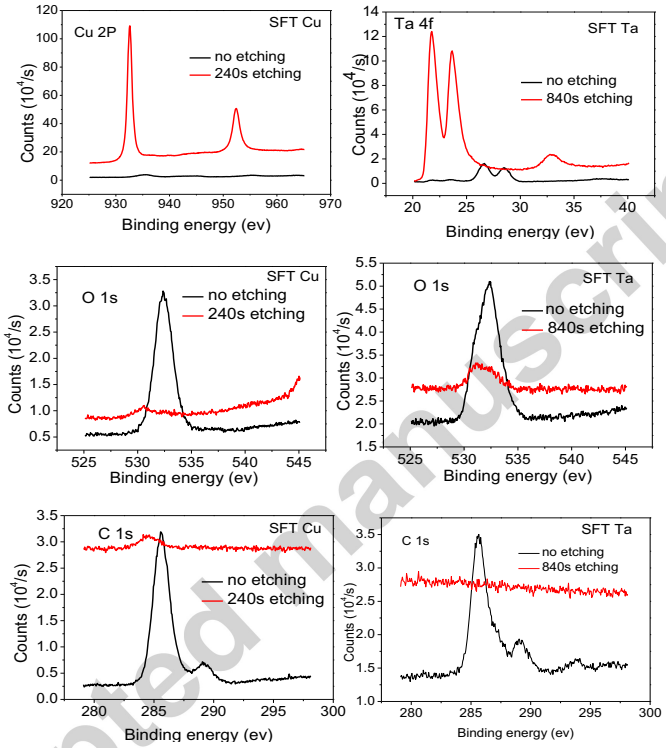


**Figure 4.** X-ray photoelectron spectra at different etching depths from the surface in the SFT Cu and Ta samples.

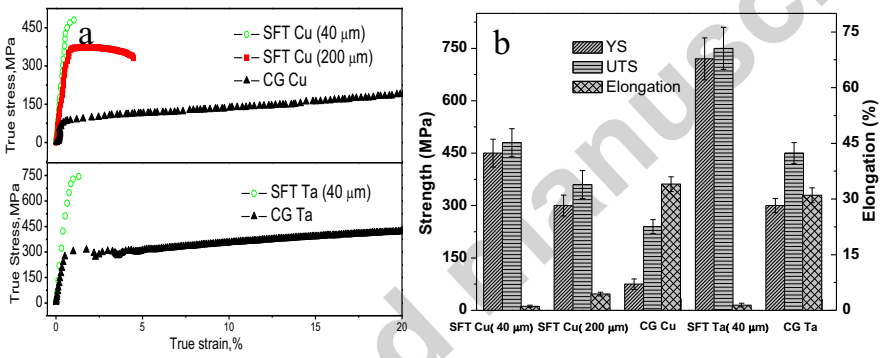


**Figure 5.** (a) Tensile true stress-strain curves and dimensions of the tensile sample (inset), and (b) summaries of the data of the surface layer in SFT samples with different thickness as indicated, in comparison with the corresponding CG samples.